Ridge Effects on Tornado Path Deviation

Nawfal Ahmed[1], R. Panneer Selvam[2]

[1,2]Department of Civil Engineering, University of Arkansas, Fayetteville, AR, 72701, USA

Abstract: **Recently few wind tunnel and computer model researchers reported that when a tornado goes over a hill the path of the tornado deviates. In this work further detailed study of the extent of path deviation for various ratios of tangential velocity to translational velocity are investigated. Wind tunnel, field and computer model data are investigated to examine the effects of topography (a ridges) on tornado path deviation (i.e. turns in tornado path while interacting with the topography). Field data from both Tuscaloosa (2011) and Mayflower (2014) tornados is considered in this study to examine effects of topography on tornado path deviation. Computer model is utilized to run six different ratios of tangential velocity to translational velocity (V_Θ/V_t) (i.e.1-4, 6, 8) and study the effects of changing this ratio on tornado path deviation. The topography shape considered in this work is a ridge. Results show that (V_Θ/V_t) ratio has significant influence on a tornado path deviation. As the ratio increases, the deviation shape changes from a straight line to single curvature then to double curvature. For ratio (V_Θ/V_t) < 2, the deviation shape is almost a straight line. For $2 \leq (V_\Theta/V_t) < 4$, the deviation shape becomes a single curvature shape. When the ratio (V_Θ/V_t) ≥ 4, the deviation shape changes to double curvature. Numerical results for (V_Θ/V_t) ≥ 4 is comparable to wind tunnel data. Therefore the computer model is considered for further investigation. The University of Arkansas (UA) computer model results for tornado path deviation shape are comparable to both experimental and field data.**

Keywords: **Tornado-terrain interaction; tornado path deviation; ridge effects on tornado path deviation; fluid-structure interaction, computational fluid dynamic.**

1.   INTRODUCTION

Tornados are a major risk for human lives and the economy. Researchers have investigated tornados in several avenues: tornado geneses, tornado forces, tornado damage, tornado path and direction, and tornado interaction with structures, etc. Early attempts have been conducted experimentally (i.e. wind tunnel) to understand tornado formation and factors affect the tornado formation and structure (e.g. [1]; [2]). A common finding is that the non-dimensional factor, swirl ratio, controls the tornado breakdown. Swirl ratio governs the vortex configuration (e.g. low swirl ratio associates with single-vortex, and high swirl ratio leads to two-cell vortex and multi-cell vortex). Furthermore, experimental tornado simulators have been employed to measure tornado force coefficients on structures (e.g. [3]; [4]).

In the numerical endeavors, Selvam and his group (e.g. [5]; [6]) have simulated tornado-structure interaction numerically. They reported tornado forces on different types of structures (e.g. circular cylinder and cubic building).

However, very little research in engineering and meteorology has been conducted to understand tornado interaction with terrain (e.g. hills, escarpment, knolls, valleys, mountains, etc.). Recently, a few studies have been carried to investigate effects of terrain on tornado path and behavior, especially after the outbreak of the Tuscaloosa tornado in 2011. Reference [7] studied sheltering efficiency of rectangular man-made walls (rectangular hills). For a wall height equal to the tornado radius, they reported that the sheltering efficiency, the ability of the structure to reduce wind velocity on its leeward side, is almost 40%. Reference [8] employed Google Earth for damage investigation of terrain effects on tornado damage. Their focus was tornado damage uphill and downhill as well as sheltering on the leeward sides of hills. They reported that there is no damage in a region surrounded by hills located on the tornado path. In these studies, no attention was paid to terrain effects on tornado path deviation, instead only damage is monitored.

Reference [9] implemented the immersed boundary method and large eddy simulation (LES) to simulate tornado in 3D domain and study the effects of topographical shapes (ridges, knolls, valleys, ridge pairs, ridges with gaps, etc.) on tornado near-surface wind. For different topographical shapes, different path deviations and pressure values are observed.

Page | 273

However, tornado radius and velocities and topography dimensions are not reported in [9]. Therefore, it is not considered for results comparison in this work. Reference [10] utilized the Iowa State University (ISU) tornado simulator to determine the effects of idealized topographical obstacles (ridges and escarpments) on tornado characteristics. They noticed that tornados experienced deviation from the center line while climbing up and down the topographical obstacles. However, the mechanism causing this behavior is not clear yet. Many parameters are involved in the tornado-terrain interaction, and much more research still need to be done for better understanding of terrain effects on tornado damage and path deviation.

In this work, ridge effects on tornado path deviation is further investigated. First, wind tunnel data presented by [11] and [10] is analyzed. Then, data collected from Google Earth for the Tuscaloosa-2011 tornado and from field investigation for the Mayflower-2014 tornado are studied to determine topography effects on tornado path deviation. A connection between the ratio of the tornado's tangential velocity to the translational velocity (V_Θ/V_t) and the path deviation shape is noticed. Since the ratio (V_Θ/V_t) is not directly provided for both wind tunnel and field data, the University of Arkansas (UA) computer model is utilized to determine the effect of changing (V_Θ/V_t) on tornado path deviation as well as to validate the computer model by a comparison with the wind tunnel and field data. There are several factors that may affect tornados' path deviation, many of these factors are associated with topography interactions (including topography height, aspect ratio and roughness of the topography, tornado size and type, intensity and translation speed) and others independent of topography. In this study, only the effect of changing (V_Θ/V_t) when tornado interacts with a ridge is studied. In addition, the UA computer model is used to visualize the flow features when a tornado interacts with a ridge and explain why the deviation happens. Knowing the tornado path might lead to better measurements of tornado velocities near the ground and better ways to track tornados.

2. OBJECTIVES

The objective of this work is to determine ridge effects on tornado path deviation, and this is addressed as follows.

- Analyze tornado path deviation due to interaction with topographical obstacles utilizing wind tunnel and field data.

- Utilize computer model to study the effect of changing the ratio (V_Θ/V_t) on tornado deviation shape when the tornado radius equals the ridge height.

- Compare the numerical results with wind tunnel data to validate the numerical model for further applications.

- Use the computer model for visualizing the tornado ridge interaction and explain why the deviation happens.

3. WIND TUNNEL OBSERVATIONS FOR TORNADO PATH DEVIATION (TORNADO-RIDGE INTERACTION)

Reference [10] utilized the Iowa State University (ISU) tornado simulator to study tornado interaction with different topographical configurations (e.g. ridges and escarpments). The simulator is a huge transferrable chamber with a fan and vanes to generate the tornado. Details of the simulator are reported in [4]. The wind tunnel experiment setup for tornado interaction with topography is presented in details in [11]. The ridge height is held fixed equal to 0.285 m. the tornado radius used is in range (0.23-0.56) m, so the simulated tornado average radius is assumed to be equal to the ridge height. The ridge profile is shown in Fig. 1a which is adopted from [11]. The maximum slope for the ridge is 20%. Details for the simulated tangential velocity values are not reported; however, Reference [4] is referred to for these details. Reference [11] reported that translational velocity used is 0.2 ms-1. Based on his setup for the simulator, tangential velocity average is estimated to be 9 ms-1. Therefore, the ratio (V_Θ/V_t) used in their simulation is estimated to be equal to 45. The minimum pressure on the ridge surface was acquired while the simulated tornado interacted with the ridge. The minimum pressure on the ridge surface due to the tornado crossed is shown in Fig. 1b. From Fig. 1b, one can see that the tornado experienced deviation in its path while climbing up and down the ridge. This deviation is defined as a double curvature deviation with two maximum eccentricities on both sides. The first eccentricity is almost at one third of the way up ridge, and the second one is at 20% of the way down ridge. Reference [11] reported that translational velocity could not be maintained constant, and that might affect the outcome. Also, the energy is provided continuously for angular momentum in the tornado's upper forcing, while a real life tornado experiences energy loss due to either interaction with structures or topography causing destruction. This might make their results differ slightly from real tornado behavior. Therefore, the topography effect on tornado path deviation is investigated for two real life tornados as discussed in the next section.

4.   FIELD OBSERVATIONS FOR TORNADO PATH DEVIATION (TORNADO-HILL INTERACTION)

In this section, the Google Earth damage path of Tuscaloosa-2011 tornado [8] and the field data of Mayflower-2014 tornado [12] are considered for investigating topography effects on tornado path deviation. In both these tornado sites, tornados interacted with hilly terrain (a terrain which has several consequent hills or any other topographical configurations in certain regions).

4.1. Tuscaloosa-2011 tornado:

Tuscaloosa-2011 is considered as one of the deadliest tornados in the last five decades. The whole path of approximately 142 km (88 miles) is shown in Fig. 2. The tornado traveled from southwest to northeast as indicated by the yellow arrow in Fig. 2. About 29km (18 miles) northeast of Tuscaloosa on the tornado path, a close up view is shown in Fig. 3. Fig. 3 illustrates the tornado signature over the hilly terrain as a light brown color. Two sites are selected with zoomed views and elevation profiles in this hilly area. For both locations, notations are given as H1 (Hill1) and H2 (Hill2) respectively. The average radius for the tornado core is estimated about 75m (246 ft) from the damaged path using Google Earth measuring tools (maximum reported damaged width is about 2.4km (1.5 miles)). The tornado maximum intensity for Tuscaloosa-2011 is EF4 with maximum velocity of 306kmh-1 (190 mph) as reported in National Weather Service report [13]. This velocity can be overestimated since it is evaluated depending on straight wind damage. The ratio of tangential velocity to translational velocity (V_Θ/V_t) is almost (3) as detected from [13]. However, due to interaction with the hilly terrain, tornado loses energy and its intensity changes as shown in Fig. 4. Fig. 4 demonstrates tornado damage path and intensities for the same region of H1 and H2 mentioned above. Therefore, the ratio (V_Θ/V_t) for this specific location is estimated to be less than two depending on the reported intensity and average traveling speed for the tornado. The height of H1 is almost 21m (70 ft) as illustrated in the elevation profile in Fig. 5, and the maximum slope is 32%. The other hill (H2), also located on the tornado path has maximum height of 18m (60 ft) (See Fig. 6).

The damaged path in Fig.s 5 and 6 is margined by dashed yellow arrows. From the close-up view for the hill (H1) shown in Fig. 5, one can see that the tornado crossed the hill with no curvature in its path. Also, the tornado with aforementioned intensity passed over the H2 with no curvature in its path as shown in Fig. 6. In other words, there is no deviation from the original path as one can see from the provided data. Furthermore, Fig. 4 confirms that tornado damage path (red area) is almost straight (No curvature) even though the terrain is hilly. In this case, the (V_Θ/V_t) ratio is estimated to be less than two, and it is interpreted to be connected with no curvature in the tornado path. Also, the hill height, slope and the shape might affect the deviation pattern. Tornado-topography interaction is abroad topic, and only the effects of changing (V_Θ/V_t) on tornado path deviation when tornado interacts with a ridge has height equals to the tornado core radius is investigated in this study.
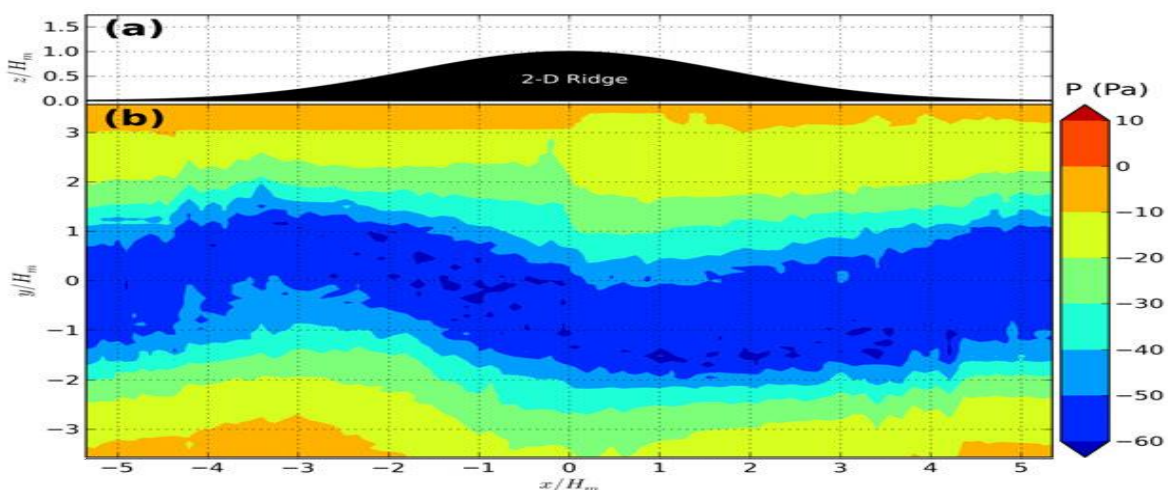

Fig. 1 a) Ridge profile b) minimum pressure on ridge surface ($V_\Theta/V_t \approx 45$) double curvature, (taken from [11])
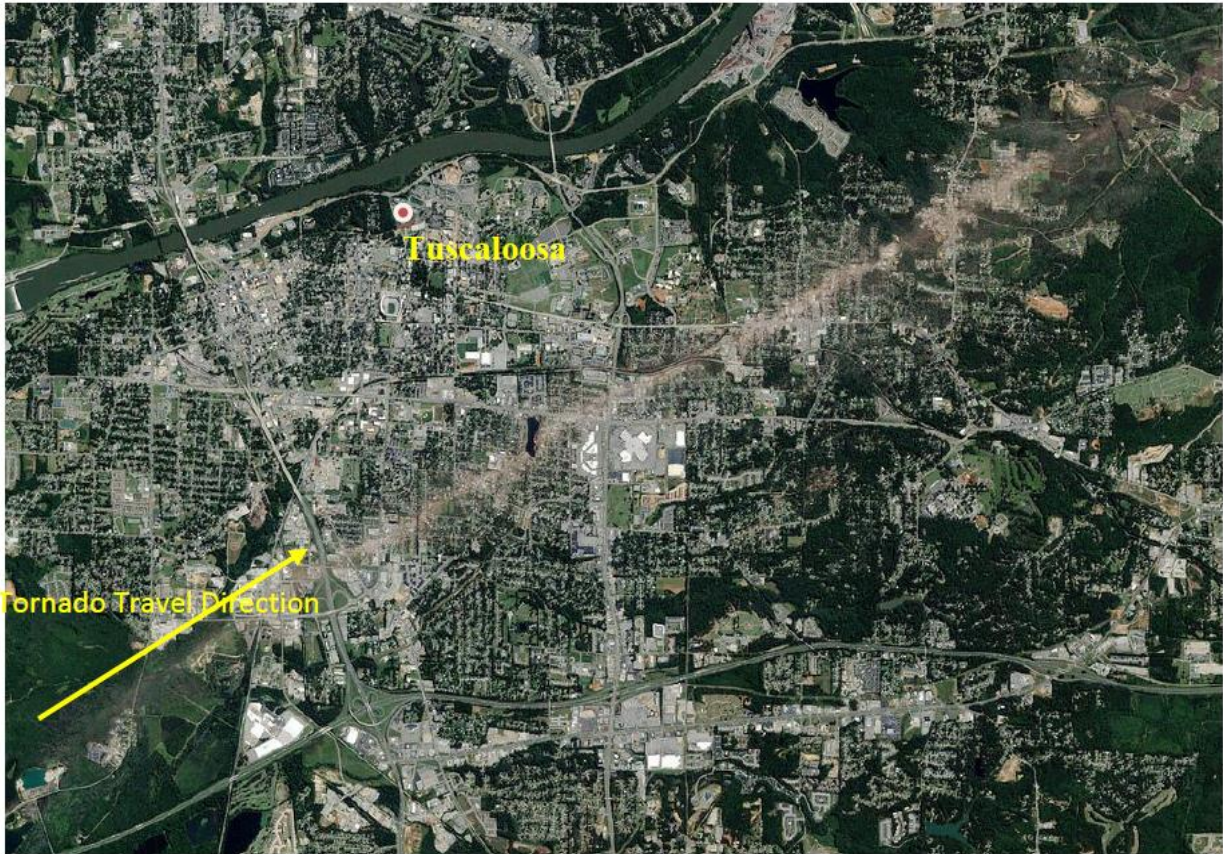
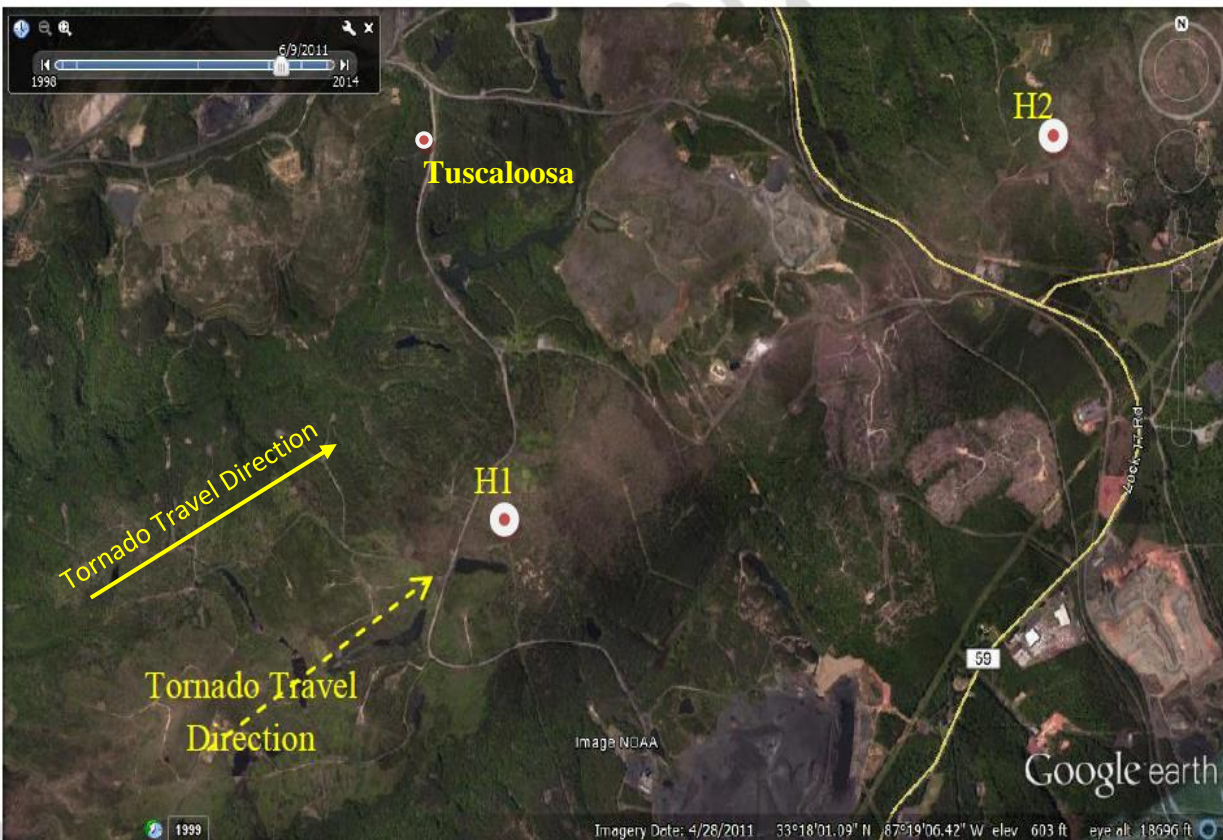**Fig. 2 Damage path for Tuscaloosa-2011 tornado adopted from [14]**

Fig. 3 Close-up view for a hilly terrain region 29 km miles NE Tuscaloosa
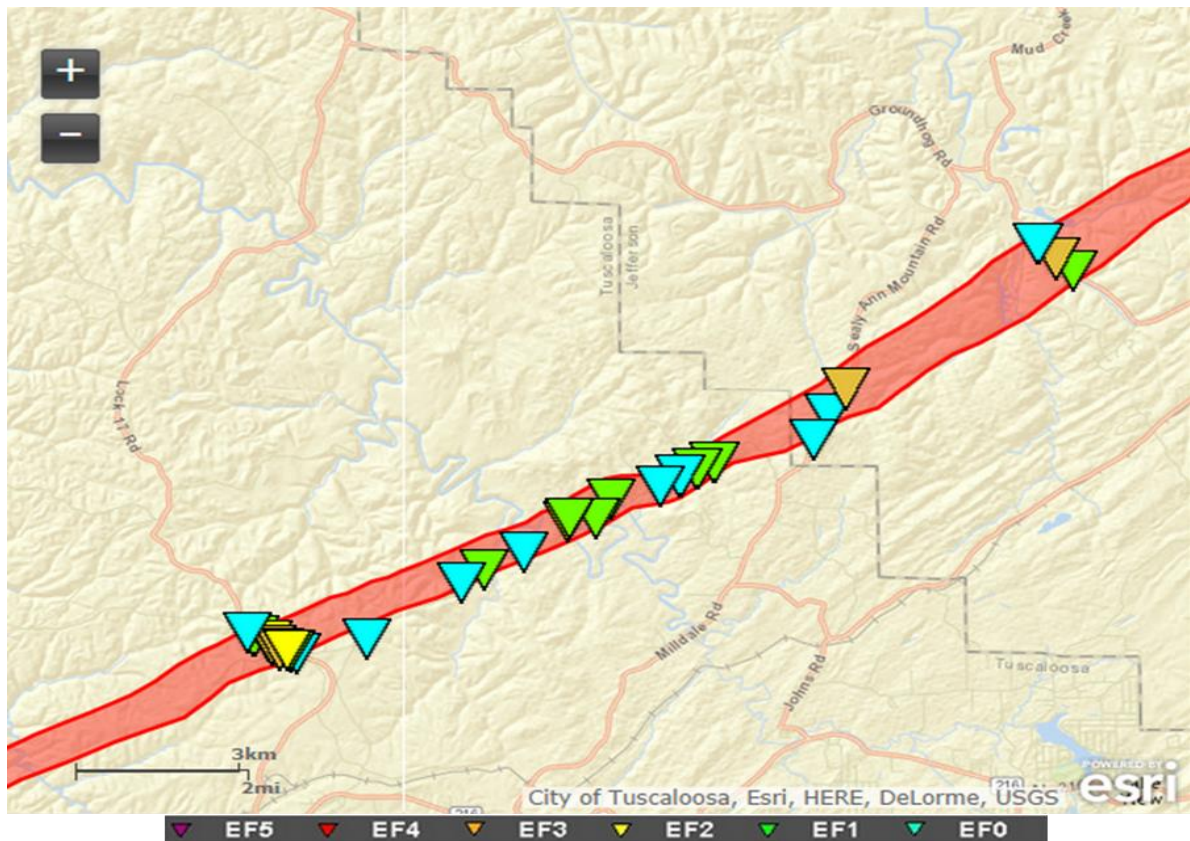
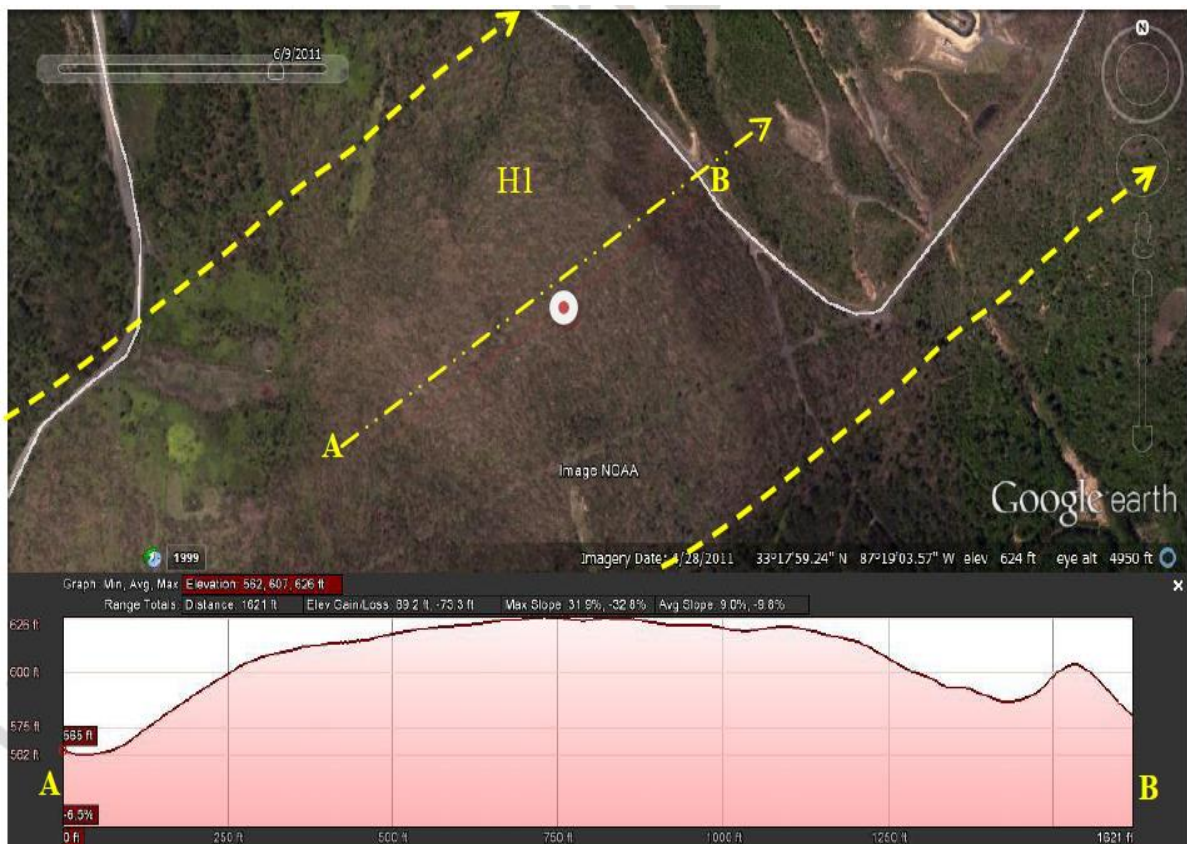**Fig. 4 Tornado intensities and damaged path for the region of H1 and H2, [13]**

Fig: 5 Close-up view and elevation profile for the hill in location H1, $(V_\Theta/V_t \approx (1\text{-}2))$. Straight line path, not much deviation noticed
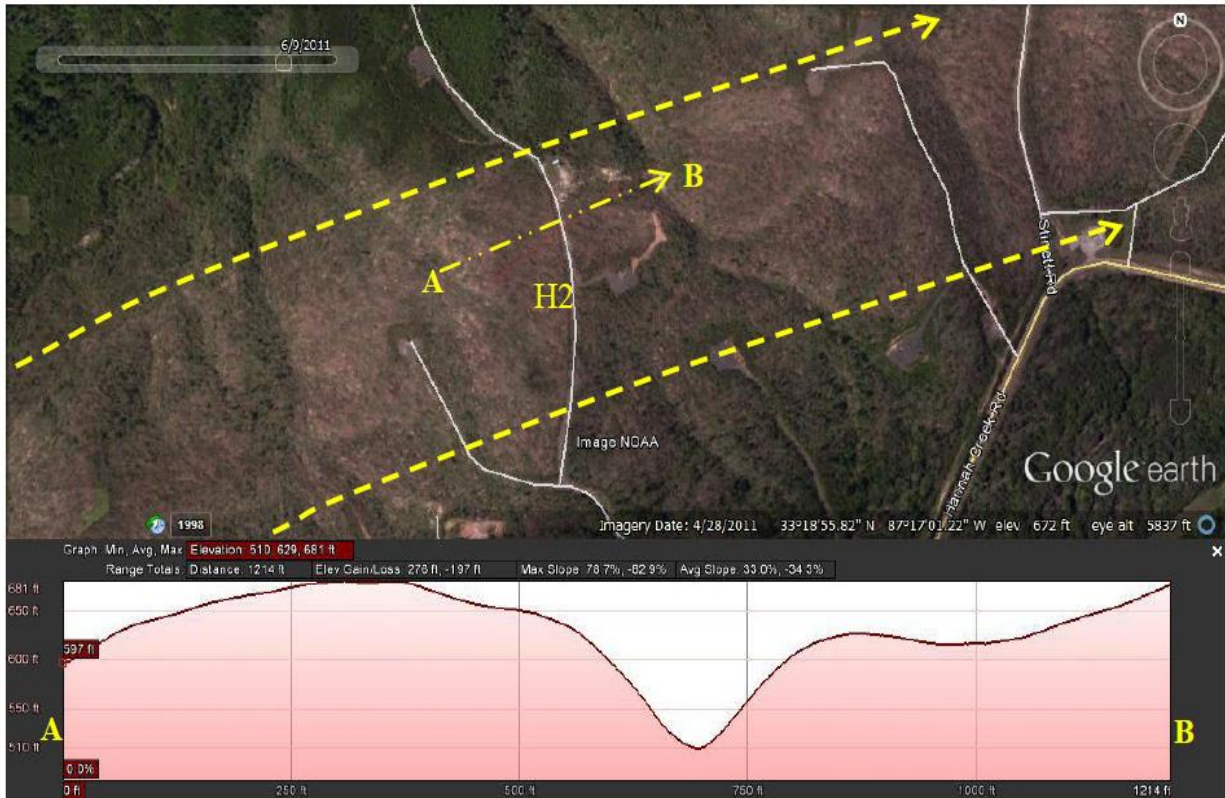
Fig. 6 Close-up view and elevation profile for the hill in location H2, ($V_\Theta/V_t \approx (1\text{-}2)$). Straight line path, not much deviation noticed

4.2. Mayflower-2014 tornado:

Another tornado event, Mayflower-2014, is selected for this study as shown in Fig. 7, an image reported by the National Aeronautics and Space Administration (NASA) [15]. The terrain in this area is also hilly, but data availability and quality are very limited. One location close to Lake Conway is studied in this site. As reported by [16], the tornado intensity varies greatly in this location between EF0 to EF2. However, there are few places with intensity of EF3 and EF4 as reported by [16]. The point here is that tornado intensity changes as tornado interacts with terrain. Rough terrain weakens tornados, while smooth terrain strengthens tornados [12]. Therefore, the ratio (V_Θ/V_t) may change slightly depending on the terrain nature. The maximum ratio of (tangential/ average translational velocity) for this site is estimated to be about (5). The tornado traveled about 64km (40 miles) in one hour as reported by [16], so Vt is estimated to be 64kmh-1 (40mph).

In the selected location, H3, the tornado passed over a water surface, Lake Conway, before it interacted with H3. Because water is considered a smooth surface, it is assumed that tornado had a high intensity. Fig. 8 shows a close-up view of the damaged path around location H3. After passing the lake, the tornado interacted immediately with a two-dimensional hill, and then hit H3 as shown in the topographical terrain image Fig. 9. Therefore, it got weakened and the ratio (V_Θ/V_t) decreased slightly. The two-dimensional hill height is about 37m (120 ft) and it is located about 0.8 km (a half mile) prior to H3. There is not enough information about the tornado core radius. However, estimation from the damaged path using Google Earth measuring tools shows that the radius is about 61m (200 ft). The NASA image is imposed on Google Earth, and then the tornado core radius is measured. Therefore, a tornado with estimated (V_Θ/V_t) ratio about (4) passed over H3. The height H3 is about 31m (100ft) as shown in the elevation profile in Fig. 10. From Fig. 10, one can see that there is a single curvature deviation from the tornado's path center line. The tornado started deviating to the right while climbing uphill to reach its maximum deviation at the hilltop. Then, it deviated back to the left while climbing down.

These two sites, Tuscaloosa-2011 tornado and Mayflower-2014 tornado, showed two completely different cases for tornado's deviation while crossing a hill. In each case the tornado had different deviation shape for different estimated (V_Θ/V_t) ratios. Therefore, computer model is utilized to verify the theory that ratio (V_Θ/V_t) affects the tornado path deviation while interacting with topography (a ridge) has a height equals the tornado radius. Also, it is used to compare

the computer results for tornado path deviation with experimental results for validation and further applications of the computer model.

Fig. 7 NASA image for the tornado path in Mayflower-2014

Fig. 8 a close-up view for location close to Lake Conway (Mayflower-2014)

Fig. 9 The terrain topography around the selected location in H3 (May flower, AR)

Fig. 10 Elevation profile for the hill in location H3, ($V_\Theta/V_t \approx 4$, single curvature).

5. COMPUTER MODEL

Tornado-terrain interaction is a complex phenomenon. However, due to huge development in Computational Fluid Dynamic (CFD) in recent years, several attempts have been conducted to clarify and understand this phenomenon. CFD promises huge advantage over experimental work due to easiness and economic cost. CFD provides full access to wind field (details of pressure and velocities) as well as allowing control of important simulation parameters.

5.1. Tornado Numerical Model:

In this work, CFD is utilized to study tornado ridge interaction with various (V_Θ/V_t) ratios. The computer data is analyzed for the tornado path deviation due to interaction with a ridge. Tornado wind field model is considered by implementing Rankine Combined Vortex Model (RCVM) which is the simplest model that satisfies Navier Stokes equations (NSEs) as reported by [17]. More details for RCVM can be found in [5]. Details for boundary conditions and implementation of RCVM can be found in [6] & [18]. The turbulence is modeled using Large Eddy Simulation (LES). Finite Elements Method (FEM) is used to approximate the NSEs. Then, the approximated equations are solved using a semi-implicit method as explained in the following section.

5.2. NS Equations Solution procedure:

The three-dimensional equations for an incompressible fluid using the LES turbulence model in general tensor notation are as follows:

Continuity Equation: $U_{i,i} = 0$ (1)

Momentum Equation: $U_{i,t} + U_j U_{i,j} = -(p/\rho + 2k/3)_{,i} + [(\nu + \nu_t)(U_{i,j} + U_{j,i})]_{,j}$ (2)

where : $\nu_t = (C_s h)2(S_{ij}^2/2)^{0.5}$, $S_{ij} = U_{i,j} + U_{j,i}$, $h = (h_1 h_2 h_3)^{0.333}$, and $k = (\nu_t/(C_k h))^2$.

Empirical Constants: $C_s = 0.1$, and $C_k = 0.094$

Where U_i and p are the mean velocity and pressure respectively. k is the turbulent kinetic energy, ν_t is the turbulent eddy viscosity, h_1, h_2, and h_3 are control volume spacing in the x, y, and z directions, respectively, and ρ is the fluid density. Here the area or volume of the element is used for the computation of h. A comma represents differentiation, t represents time, and i =1, 2 and 3 refers to variables in the x, y and z directions. For further details, one can refer to [19].

The incompressible momentum and continuity equations are solved using sequential solution procedures. In this work the following sequential procedure is used to solve the unsteady NS equations:

1-   Solve velocities using the momentum equations.

2-   Solve the pressure using the new velocities:

$$\Delta P = [\partial U/\partial x + \partial V/\partial y + \partial W/\partial z]/\Delta t - [\partial(U\partial U/\partial x + V\partial U/\partial y + W\partial U/\partial z)/\partial x$$
$$+ \partial(U\partial V/\partial x + V\partial V/\partial y + W\partial V/\partial z)/\partial y + \partial(U\partial W/\partial x + V\partial W/\partial y + W\partial W/\partial z)/\partial z]$$ (3)

Here U, V and W are the velocities in the x, y and z direction, P is the pressure over density and Δt is the time step. The above sequential procedure is a general version of the one used by [20] using least square FEM. The procedure is also similar to that reported in [21], [22] and [23] using FDM. The pressure equation is arrived at by differentiating the momentum equation by x,y and z and adding them. In the equation, higher order terms as well as the continuity equation for the current time step are dropped. This eliminates the pressure correction step suggested in [19] and [24] and hence is computationally efficient and also conducive for higher order elements. This procedure is also much stable and useful for adaptive and other techniques. When solving the equations by FDM or CVM using cell centered grids, the pressure values are solved in the fluid cell center and then the pressure is extrapolated on solid. Rather than this approach, if the pressure is solved over the solid body the accuracy is much better as discussed by [25]. The above equations are solved by FEM. Even though FEM takes more computer time the transport accuracy of the vortices are very high as reported in [23] and hence it is preferred in this work. Because of the large computing time, the model is parallelized by making subdomain in the vertical direction. The data from one processor to another is communicated using MPI. The detail of the parallel computing is reported in [26]. The equations are solved by preconditioned conjugate gradient. The computer model is ran

for 90 time units and this takes 720hrs (30days) when serial computing (one processor) is used. However, this time is reduced ten times to 72hrs (3 days) when the distributed parallel computing (24 processor, MPI) is utilized.

5.3. Computational Domain and Grid Generation:

A terrain following grid system shown in Fig. (11) is used here. Different terrain following coordinate systems are discussed in [27] and [28]. To reduce the time in grid generation, equal spacing is used in the x and y directions and almost the same spacing in the z-direction. The top boundary in the z-direction is kept far away from the ground and having the same elevation from the flat ground. The equal spacing in the horizontal directions (X&Y) helps to use the program to directly consider the coordinates from the GIS system for an actual complex terrain site. The ground elevation for each x and y point is provided as h(x,y). The desired grid spacing in the z-direction far away from the ridge is provided at one (x,y) point. In this study the z-spacing is kept constant. When the distance between the ground and the top boundary changes because of ground elevation then a proportional spacing to that of the flat ground spacing is used from the following relationship:

$$Z_K^t = h(x, y) + (h^t / h^f)(Z_K^f - Z_1^f)$$

(4)

Where hf = Zkmf- Z1f and ht = Zkmf- h(x,y) . Here the superscripts f and t refer to the reference height at the inflow and a height at any point in the domain respectively.
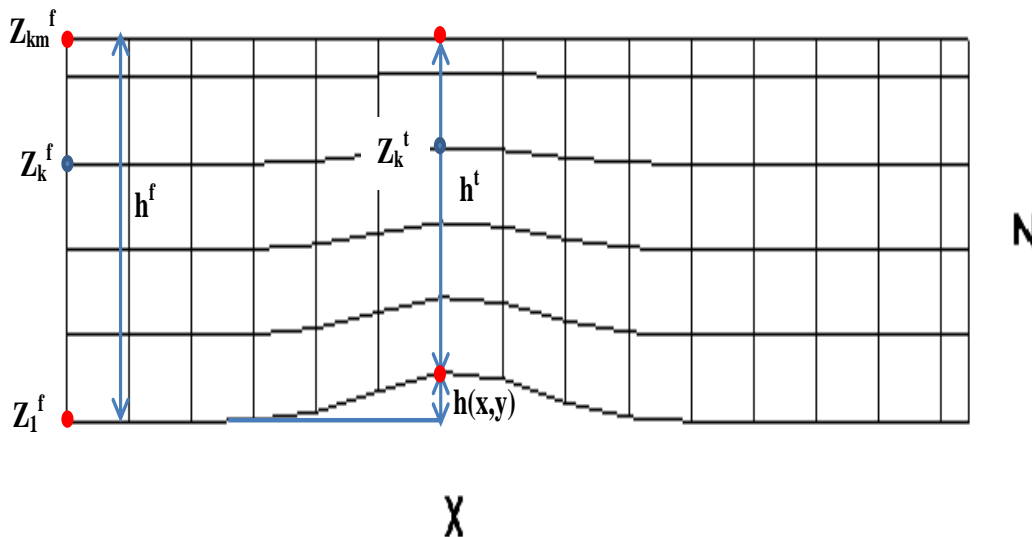

Fig. 11 notations for terrain following grid system

The computational domain considered here is 35Hx35Hx7.5H. Here H is the height of the ridge, and it equals 2 units in non-dimensional units and equals 50m (164 ft) in actual units. Here the NS equations are solved using non-dimensional values. The grid used in this study is 290x290x90 (7.569 million) points. Fig. 11a shows the grid in XZ plane, and Fig. 11b is a close-up view for the grid close to the ridge surface. The grid spacing in X, Y and Z directions are (0.1H, 0.1H and 0.085H) respectively. When unequal spacing is used in the vertical direction to capture the boundary layer accurately, there is an extensive error in the transport of the vortex. So at this time due to computational restriction a spacing of 0.085H (4.25 m) is used here.

5.4. Vortex Transportation on a Flat Terrain:

The goal here is to transport the vortex along the X axis, and monitor the minimum pressure on the numerical domain ground to study tornado's path deviation. No topography is considered for this purpose, and the vortex is transported completely along the X axis of the domain as shown in Fig. 12. Therefore, the grid of (290x290x90 points) with the aforementioned spacing is considered for the rest of this study. Even though $(V_\Theta/V_t) = 3$, one can see that the tornado path is almost a straight line in Fig. 12, because of the flat terrain (no topography effects). Also, there is 25% reduction in the width of the minimum pressure because of the loss in the vortex strength due to turbulent dissipations, but this is acceptable since only the path deviation is monitored.
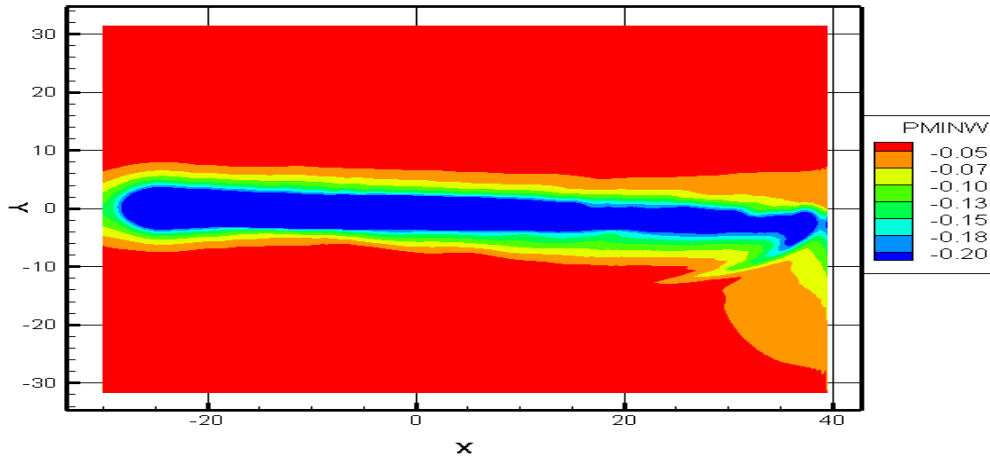
Fig. 12 Minimum pressure on the domain ground (flat domain), (VΘ/Vt) =3.

5.5. Simulation Parameters:

The tornado radius and ridge parameters used in this work are taken from [11] for a better comparison between experimental and numerical simulations. However, details for tangential to translation velocities ratio are not reported in Karstens works [11], so a range of values are considered in the model. The tornado radius is equal to ridge height, and the ridge profile is represented by the below Gaussian equation adopted from [11].

$$Z_i = H.e^{(-0.5x_i^2/500^2)} \qquad\qquad (5)$$

Where Z_i is the height at distance x_i from the center, H is the height of the ridge.

There are several factors control and affect the tornado-terrain interaction. Some of these factors are; obstacle shape profile, slope of the obstacle, obstacle height, obstacle length, ratio of obstacle height to tornado radius, ratio of obstacle length to tornado radius and ratio of tornado tangential velocity to translational velocity. In real life, there could be more factors involved. In this work, a ridge shape is used with height equals tornado radius (r_{max}), width equals 30 r_{max} and slope equal 20% as illustrated in Fig.s 13 and 14. The shape profile of the ridge, the ratios of the tornado radius to both height and length of the ridge are all fixed and used similar to those reported in [11]. The ratio of (V_Θ/V_t) observed from real tornado is in the range (1-6). In this work, the ratio of tangential velocity to translational velocity is varied within the range (1-8) to compare the results to experimental and field data as well as to verify its effects on tornado's path deviation. Tornado radius (r_{max}) equals 2 units and a ridge height of 2 units are used in this work. Table 1 illustrates parameters used in the wind tunnel experiment by [11], University of Arkansas (UA) numerical simulations and that estimated for field data. In Table 1, values of velocities and tornado radius for numerical and experimental simulations are normalized with respect to ridge height (H). Numerical domain and pressure Iso-surface of tornado approaching the ridge is shown in Fig. 13. Fig. 14a shows the grid in XZ plane but the coarseness of the grid is increased for visualization purposes. Fig. 14b is a close-up view for the grid close to the ridge surface with all grid points drawn.
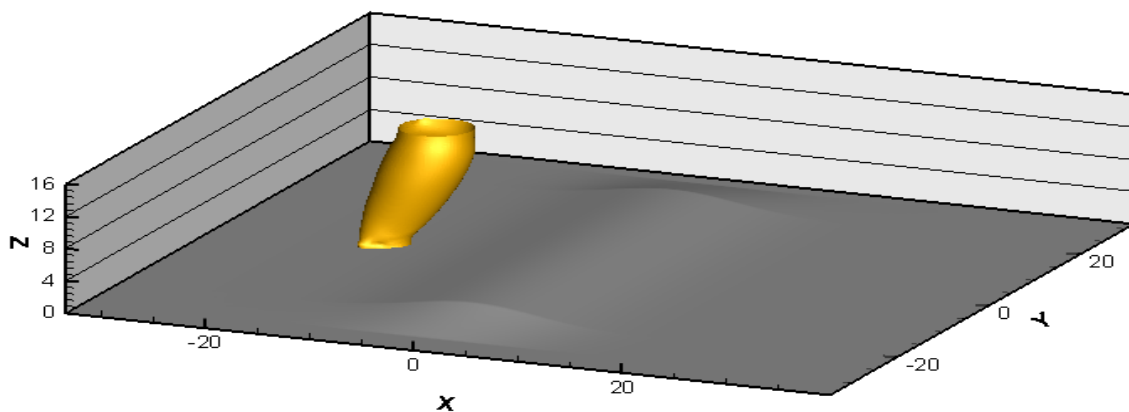

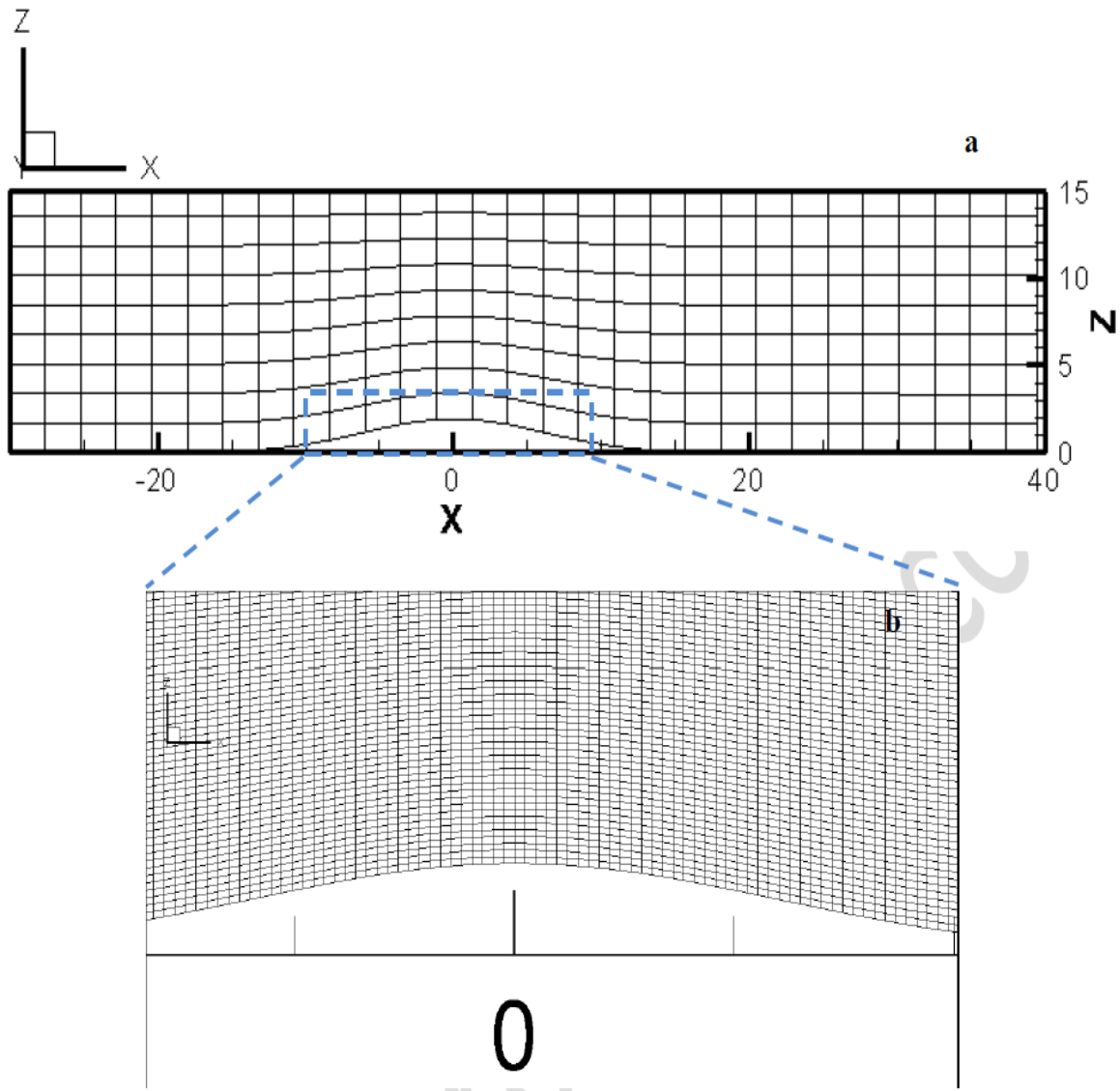**Fig. 13 Numerical domain with pressure Iso-surface approaching the ridge**

Page | 283

Fig. 14 a) Grid configuration in XZ plane (10 points skipped). b) A close-up view close to the ridge surface (all the points drawn). (Total grid point is 290x290x90)

6.   RESULTS DISCUSSION OF COMPUTER MODEL

The effect of changing the ratio (V_Θ/V_t) on tornado path deviation is investigated. Six different ratios (i.e.1, 2, 3, 4, 6, 8) are considered. These six parameters are mentioned in Table 1 as UA1 to UA6. The coordinates, in both X and Y axis, are normalized with respect to the ridge height. The outcome is striking, and it shows that there is a significant effect of changing the ratio (V_Θ/V_t) on tornado path deviation for the investigated ridge. For ratio equal to one, the path is almost straight (no deviation) as shown in Fig. 15. For ratios (2 &3), the path has tiny little bend to the left close to the center of the hill, then it deviates sharply to the right. This can be defined as single curvature as shown in Fig.s 16. When the ratio is greater than 4, one can see that the path has double curvature as shown in Fig.s 17 and 18. The ratio 6 is considered for the discussion. From Fig. 18, one can see that tornado starts to deviate left from the center line while climbing up the ridge. The maximum devition is about 0.75H when tornado reaches the top of the ridge. Then, it turns about 0.75H off the center line to the right as it goes down the ridge. After it is off the ridge, it starts to move back to the center.

6.1. Comparison of Computer Model with Field and Wind Tunnel Data:

From the aforementioned results, one can see that as the ratio (V_Θ/V_t) increases, the tornado path changes from straight line (no deviation) to single curvature then to double curvature. This gives better understanding for the mechanism responsible for this behavior as discussed later.

These results explain one of the reasons why tornados have different path shapes in different situations in real life tornados. Even though our computer parameters are not exactly similar to that in real life, it is still possible to do comparison for tornados general actions. For ratio equal to one, the result is in very good agreement with tornado path over H1 and H2 in Tuscaloosa-2011 tornado as illustrated in Fig.s 5 & 6. Also, at location H3 in Mayflower-2014 tornado shown in Fig. 10, the estimated average value for (V_θ/V_t) is about four. Therefore, it is expected to see double curvature for the path deviation if the ratio is equal or greater than four. It shows single curvature which means that the actual (V_θ/V_t) ratio in that specific location might be less than four.

The results for ratios greater than four are comparable to wind tunnel results presented by [11]. However, there is little difference in the location of the maximum deviation and the magnitude of these deviations due huge difference in the simulated ratios. Due to limitations in numerical model the simulated (V_θ/V_t) ratio in experimental work could not be consider exactly. As the ratio increase, the results are more comparable to the wind tunnel results. This means that the computer model is capable of generating reasonable tornado and can be considered for further applications and studies.

Table 1 (V_θ/V_t) for experimental, numerical and real life tornado

|	H	r_{max}	slope	V_θ	V_t	(V_θ/V_t)
Experimental Karstens(2012)	1	1	20%	31.6 unit/s	0.7 unit/s	45
Numerical UA1	1	1	20%	1.5 unit/s	1.5 unit/s	1
Numerical UA2	1	1	20%	1.5 unit/s	0.75 unit/s	2
Numerical UA3	1	1	20%	1.5 unit/s	0.5 unit/s	3
Numerical UA4	1	1	20%	1.5 unit/s	0.375 unit/s	4
Numerical UA5	1	1	20%	1.5 unit/s	0.25 unit/s	6
Numerical UA6	1	1	20%	1.5 unit/s	0.185 unit/s	8
Mayflower tornado	1	2	~32%	1 unit/s	0.21 unit/s	4.75
Tuscaloosa tornado	1	4.1	~26%	1 unit/s	0.31 unit/s	3.2
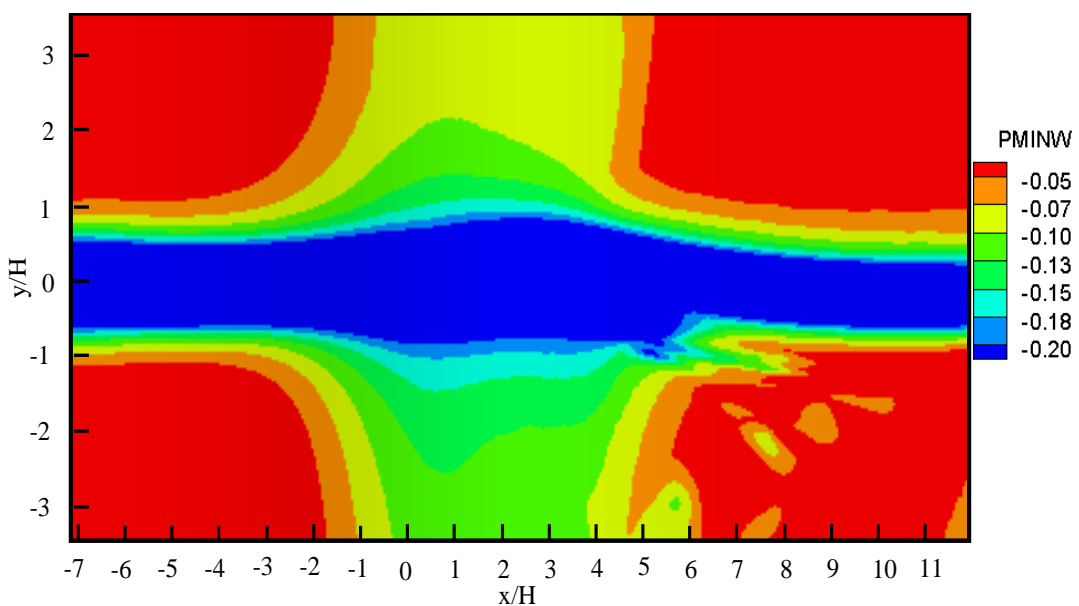
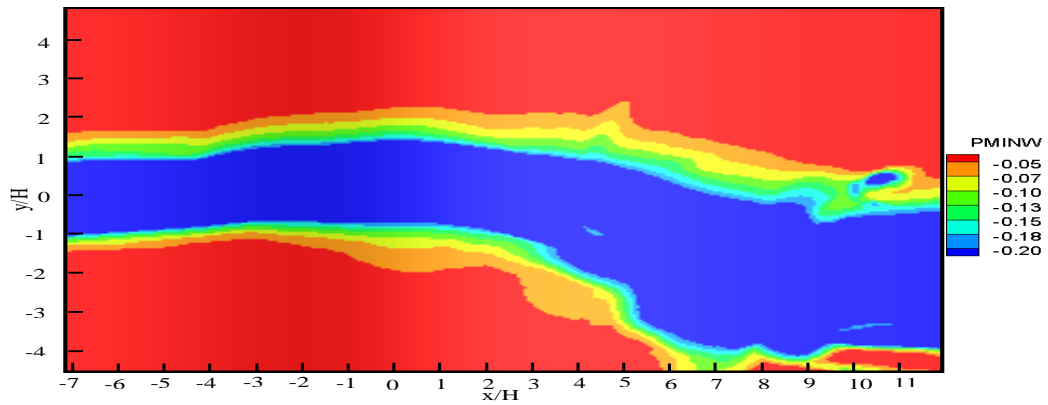**Fig. 15 Minimum pressure on 2D ridge surface for $(V_\theta/V_t=1)$, no deviation (straight line).**

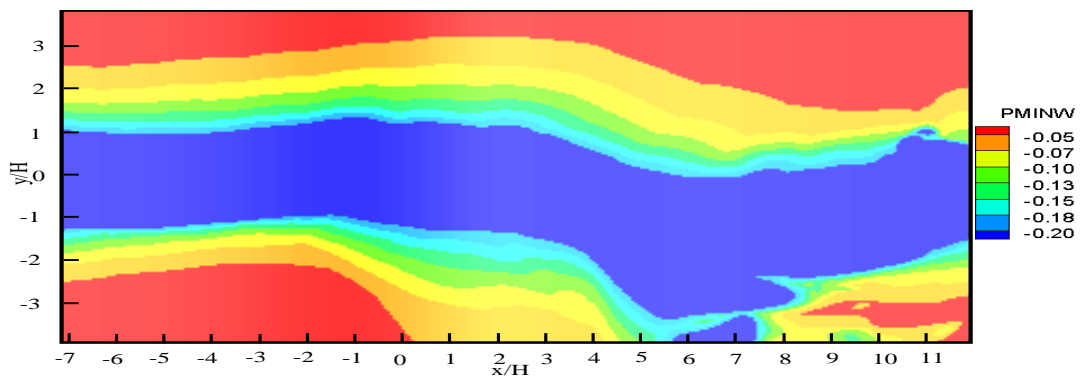**Fig. 16 Minimum pressure on 2D ridge surface for (V_Θ/V_t=2), single curvature.**

Fig. 17 Minimum pressure on 2D ridge surface for (V_Θ/V_t=4), double curvature.
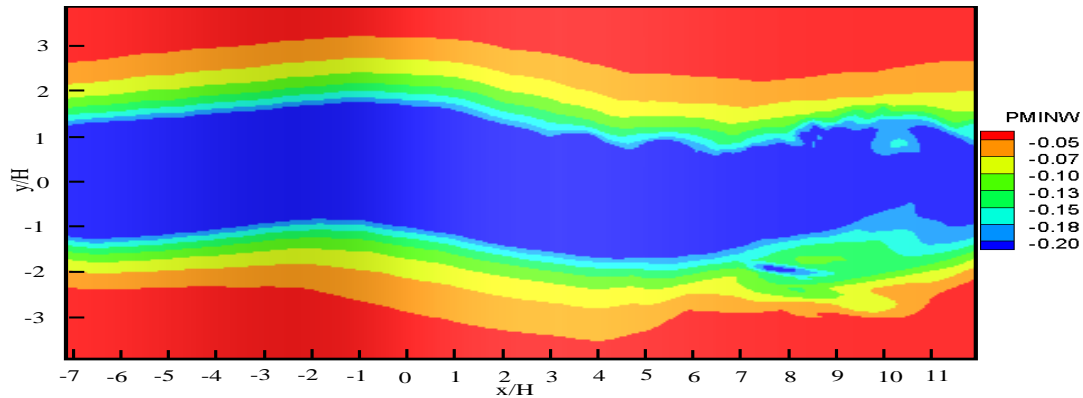

Fig. 18 Minimum pressure on 2D ridge surface for (V_Θ/V_t=6), double curvature.

7. DEVIATION ANALYSIS

In this section an explanation of why tornado deviates while interacting with topography is sought. First, it is important to make the terminology used here clear and easy to follow. The tornado is transported along the X-axis in the numerical domain as it is mentioned early. Therefore, any deviation in the tornado path is going to be either on the positive side (left) or the negative side (right) along Y-axis. Different 2D and 3D views are used to interpret the tornado deviation, and in all these views the term (left) is used whenever the tornado deviates toward the positive Y, and the term (right) is used whenever the tornado deviates toward the negative Y. The ratio (V_Θ/V_t =6) is considered in this section. The pressure contours for two slices in the YZ plane are drawn in 2D and 3D to make our terminology clear and show the tornado deviation. Fig. 19a shows 3D view for the pressure contours for a slice in YZ plane at position (X=-5) while the tornado is climbing up the ridge. From Fig. 19a, one can see the tornado tilts toward the left (+Y). The 2D view of the same slice is shown in Fig. 19b and it shows that there is clear deviation to the left. Similarly Fig. 20 a&b show the tornado deviates toward the right (-Y) while the tornado is moving down the ridge. The pressure iso-surface for the tornado while climbing

Page | 286

up the ridge and going down the ridge is illustrated in Fig. 21 a&b. From Fig. 21, one can see that the tornado base is not level as long as the tornado on the ridge surface. This creates channeling effects and makes the tornado deviates. The velocity vectors are drawn at two the locations shown in Fig. 21 a&b for better explanations. The velocity vectors are plotted in the horizontal plane (XY) as shown in Fig. 22a to visualize the guiding velocities direction while the tornado moving up the ridge. From Fig. 22b, one can see that velocity vectors toward (+Y) left (red vectors) are much more than that in the opposite direction (blue vectors), and that finally makes the velocity magnitude leads the tornado toward the left as shown in Fig.22c. On the leeward side of the ridge (Fig. 23a), one can see that the channeling effect is governing the flow to the right (-Y). Velocity vectors in the XY plane on the way down ridge are shown in Fig. 23a where the velocity vectors (red vectors) toward the left (+Y) are very less comparing to the ones pushing towards the right (blue vectors) as shown in Fig. 23b. Therefore, the tornado is guided toward the right by the resultant velocity vectors as shown in Fig. 23c. For low (V_Θ/V_t) ratio, the translational velocity is high, and it controls the tornado toward the forward direction.
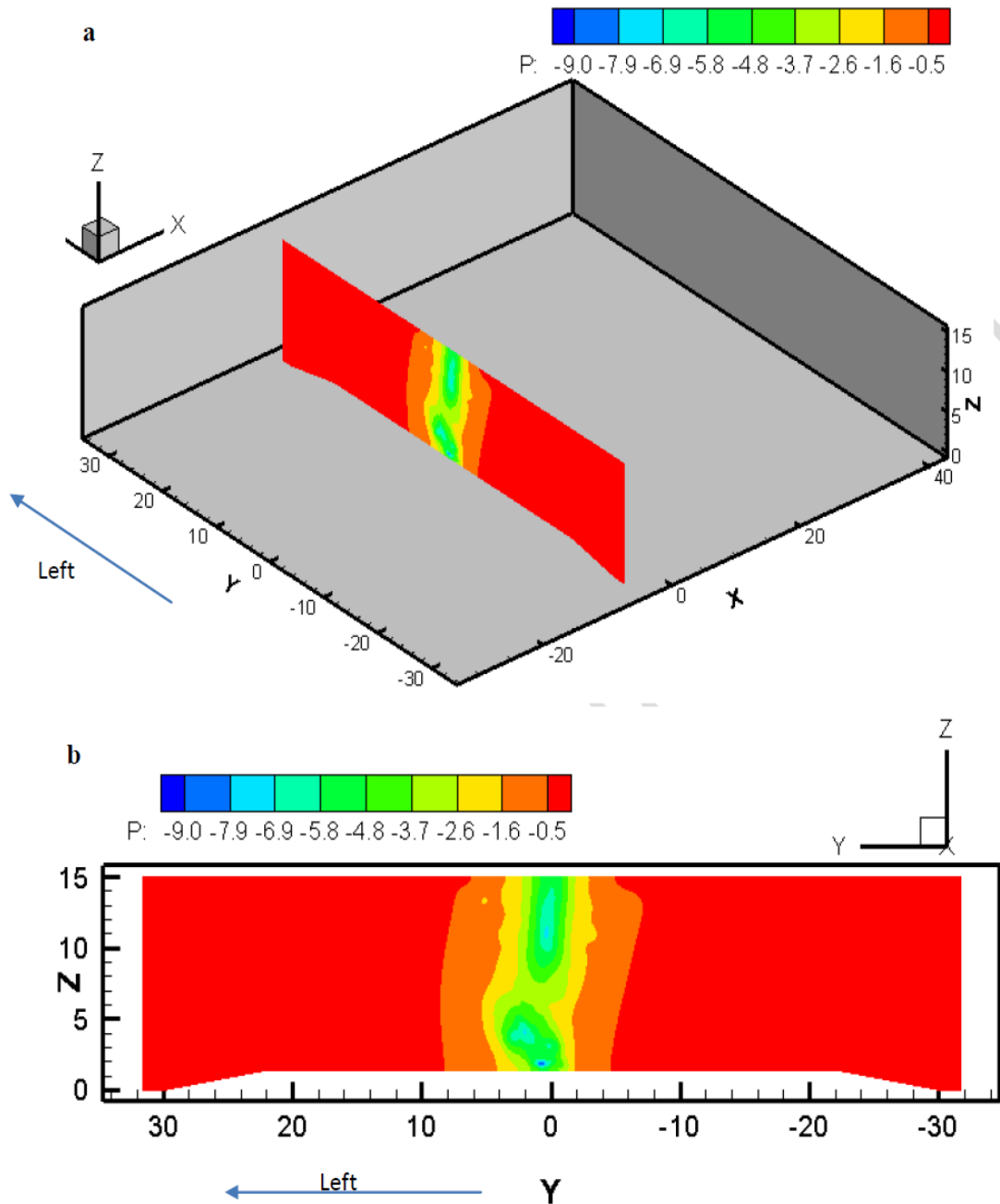

Fig. 19 tornado deviation toward the left (+Y) while climbing up the ridge a) a 3D view for the pressure contours of a slice in YZ plane b) a 2D view of the same slice
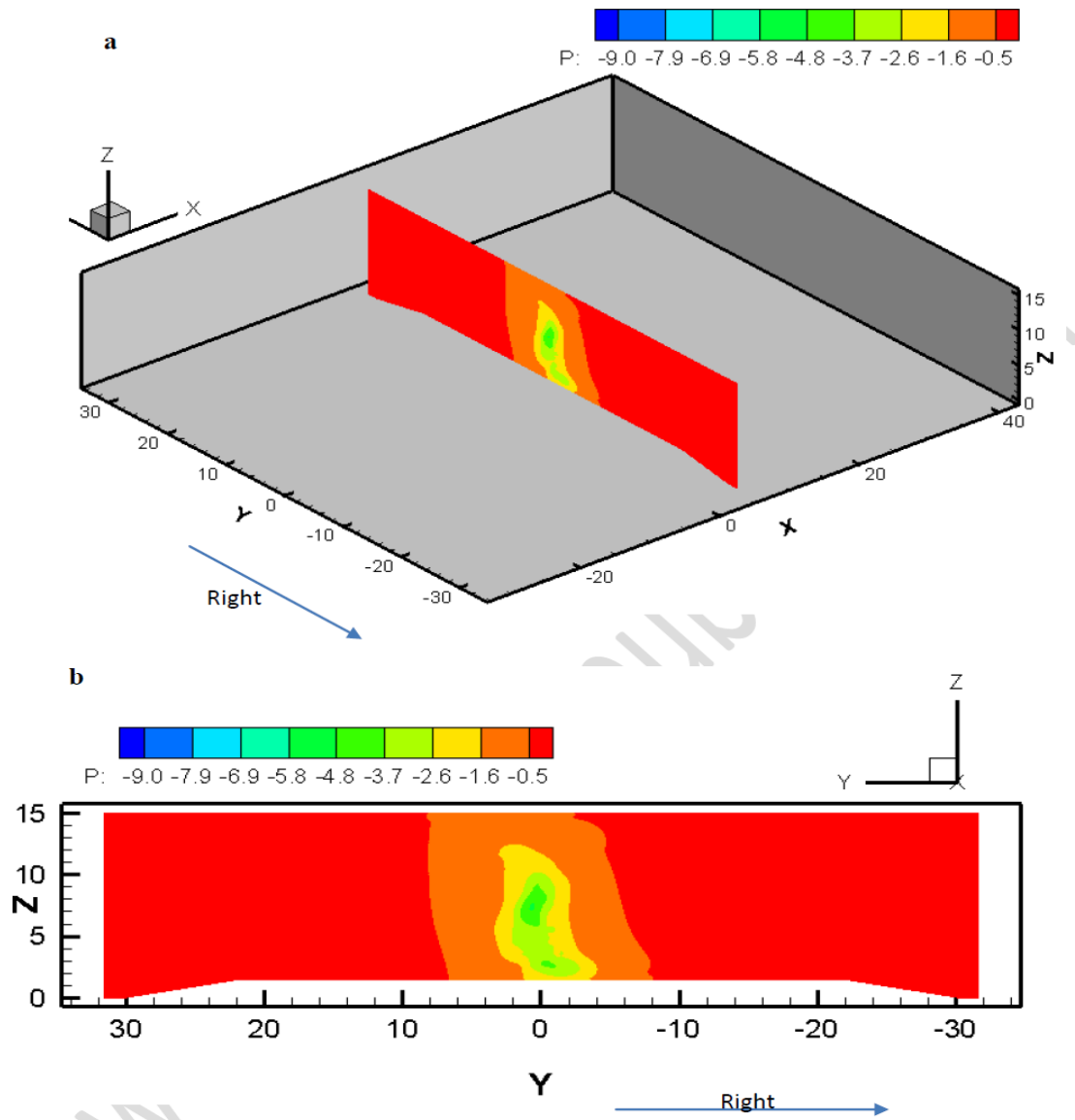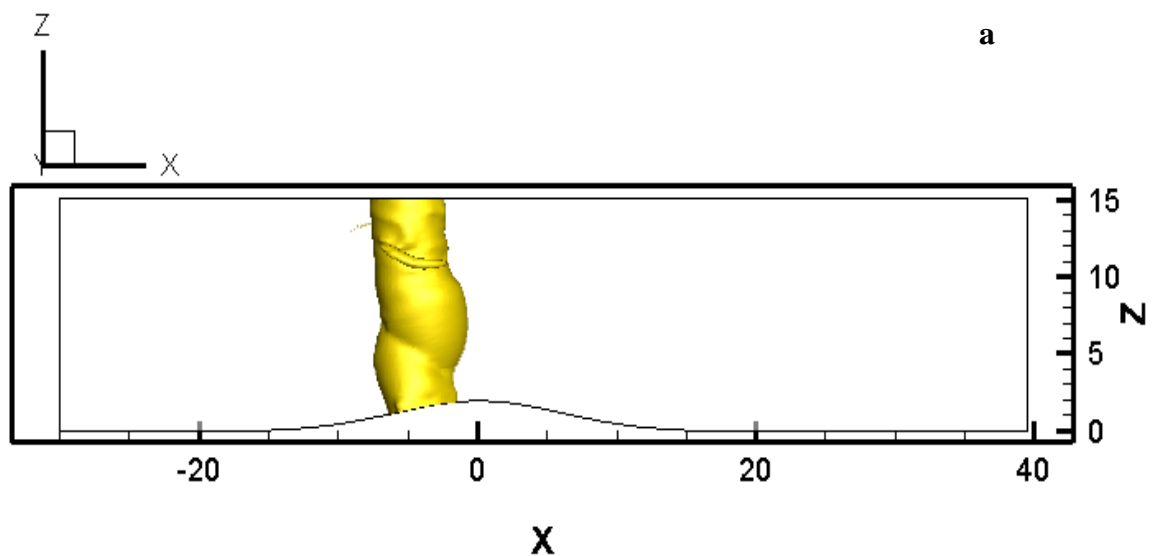
Fig. 20 tornado deviation toward the right (-Y) while moving down the ridge a)3D view for the pressure contours of a slice in YZ plane b)2D view of the same slice.
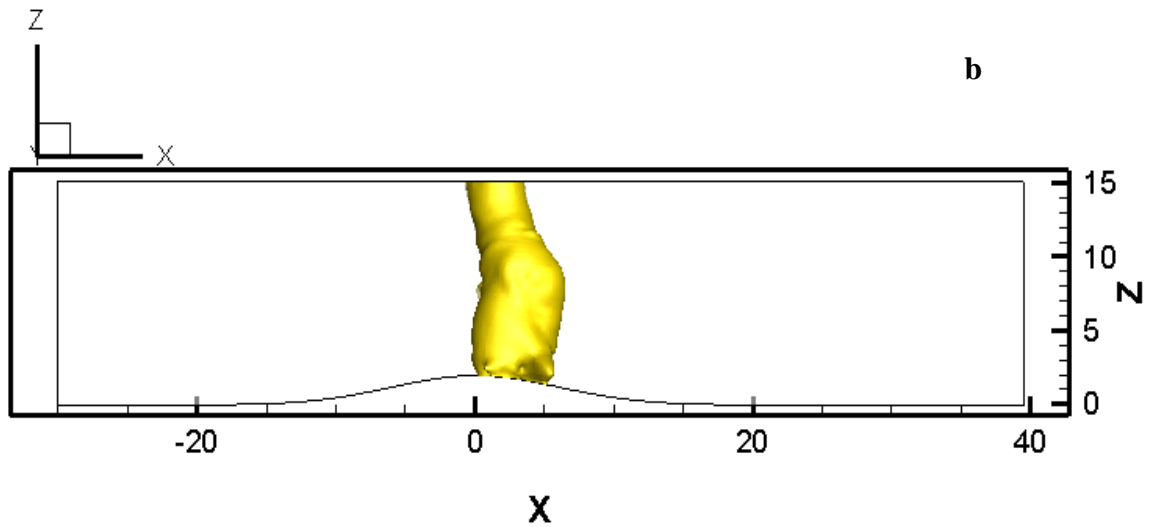
Fig. 21 Pressure Iso-Surface of the tornado a) climbing up the ridge b) moving down the ridge.
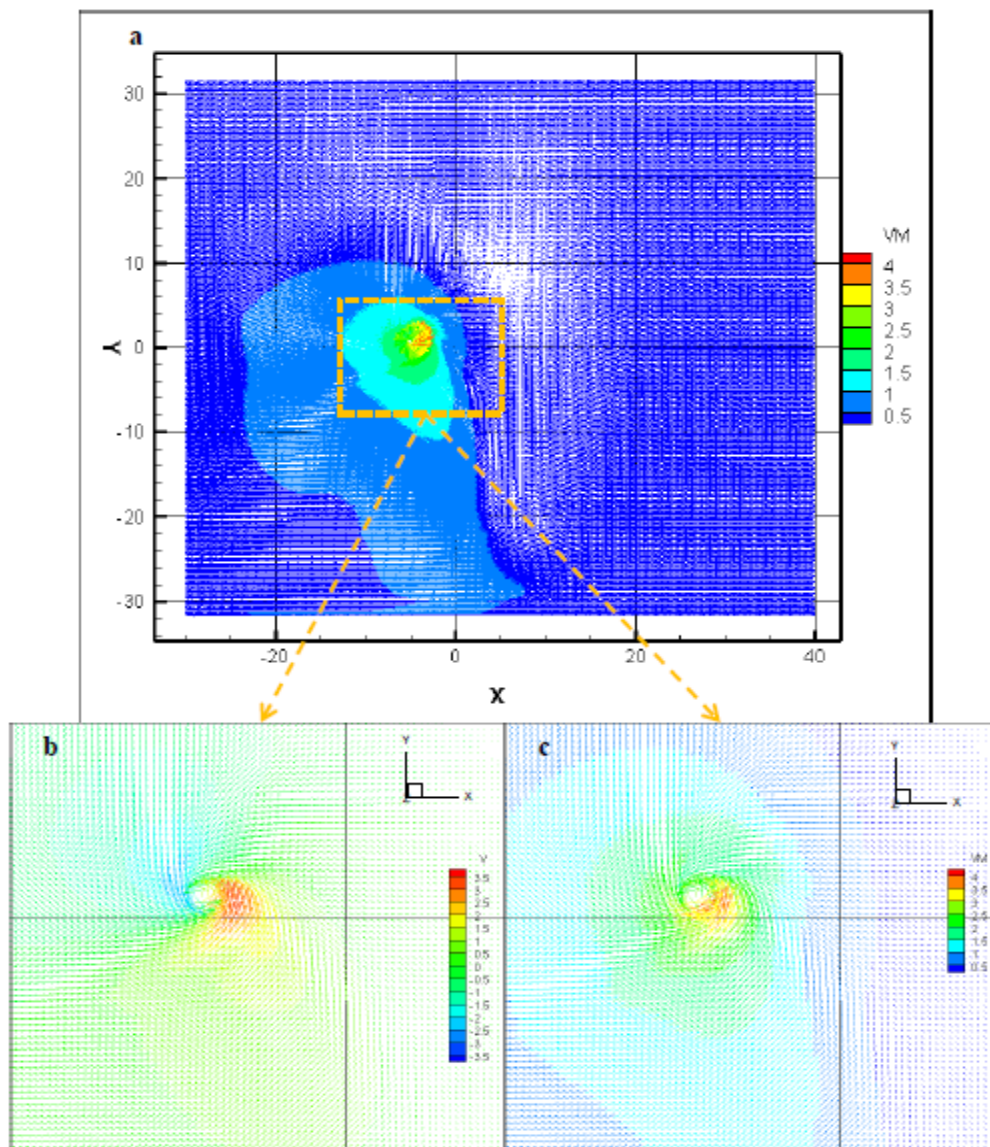

Fig. 22 Velocity vectors while climbing up the ridge a) Velocity magnitude vector for the whole domain b) close up view for velocity vectors in y direction c) close up view for velocity magnitude vectors $(V_\Theta/V_t=6)$
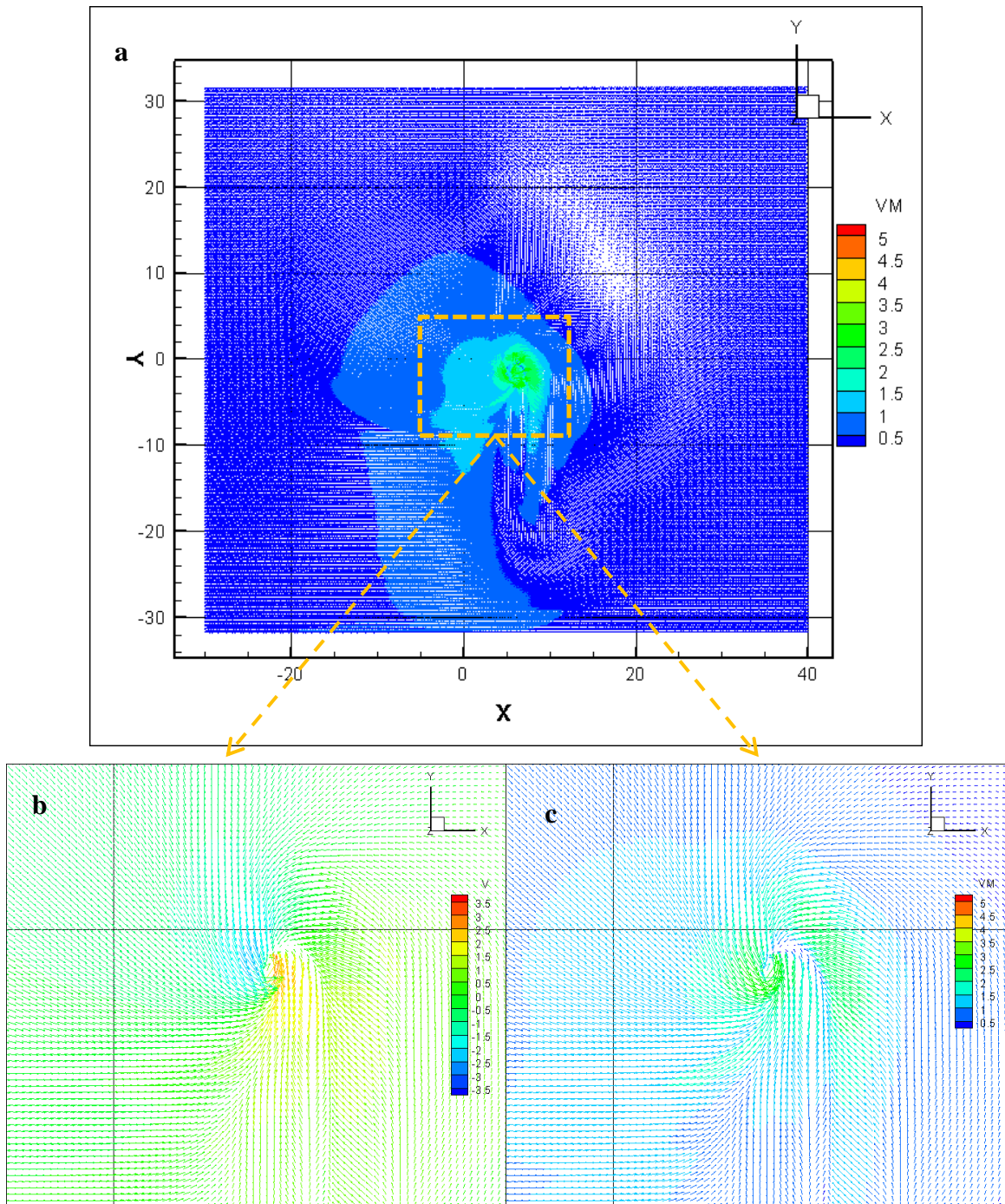
Fig. 23 Velocity vectors while climbing down the ridge a) Velocity magnitude vector for the whole domain b) close up view for velocity vectors in y direction c) close up view for velocity magnitude vectors ($V_\Theta/V_t=6$)

8.   RESULTS SUMMARY

With the existing three different sources of data, wind tunnel data, field data and computer results, it is shown that (V_Θ/V_t) ratio is one of the factors responsible for tornado path deviation. First, from wind tunnel and field data (H3 on Mayflower-2014), it is shown that for higher velocity ratios, there is more deviation (single and double curvature). Then, from field data (H1& H2 on Tuscaloosa-2011) using Google Earth data, it is shown that there is not much deviation (no deviation almost a straight line) for low ratios. By using the computer model, the influence of various ratios are predicted and compared. The comparison shows that as the ratio increases the path deviated more. Fig. 24 shows different tornado paths associated with its traveling speed as reported by [29]. It shows that slow tornado, high (V_Θ/V_t) ratio, experiences path deviations while traveling. Also, it shows that fast tornados, low (V_Θ/V_t) ratio, move in straight lines (no deviation). However, in [29], no attention was paid to topography effects. In all the aforementioned results, the effect of a ridge

whose height is equal to tornado radius is considered on tornado path deviation for various (V_Θ/V_t) ratios. However, the field data shows that topography height has an effect on tornado path deviation. After crossing the Arkansas River 3.5 miles south west Mayflower, the tornado travels over almost flat terrain until it hits the interstate I65 (part of I40) as illustrated by Fig. 25 taken from Civil Air Patrol [30]. The interstate I65 location and elevation is illustrated by using Google Earth as shown in Fig. 26. The tornado created severe damage at I65 region, so it had high intensity before it coincided I65. However, due to low height for I65, just few meters (2 m) above the surrounding ground, it does not affect tornado path. The same behavior also noticed when the tornado with ratio (V_Θ/V_t) equal to (3) is transported over flat terrain as illustrated in Fig. 12. Further understanding of the influence of ridge height, ridge length along the tornado path or the influence of the slope needs to be investigated.
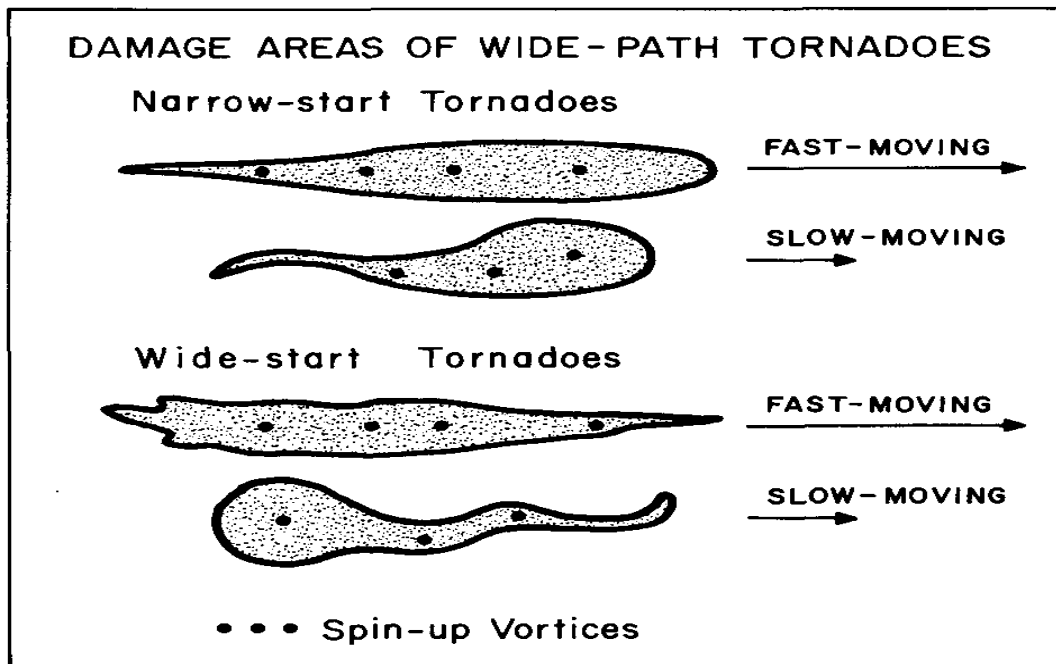

Fig. 24 Tornado path configuration associated with its traveling speed taken from [29]

Fig. 25 Tornado path at I40 showing no path deviation, ($V_\Theta/V_t \geq 4$, but low hill height) adopted from [30]

Fig. 26 Elevation profile for line AB at interstate I40 where it is hit by the tornado.

9.   CONCLUSIONS

The ridge effect on tornado path deviation is investigated using three sources of data (i.e. Field Data, Wind tunnel data and Computer simulations). For a ridge height equals the tornado radius, only the effect of changing the ratio (V_θ/V_t) is studied. The following conclusions are drawn.

• The ratio (V_θ/V_t) is a significant factor that affects the tornado deviation shape and magnitude when interacts with a 2D ridge.

• For the investigated ridge, the curvature changes from straight line to double curvature shape as the ratio (V_θ/V_t) increases.

• For ratio $(V_\theta/V_t) < 2$, the deviation shape is almost a straight line. For $2 \leq (V_\theta/V_t) < 4$, the deviation shape becomes a single curvature shape. When the ratio $(V_\theta/V_t) \geq 4$, the deviation shape changes to double curvature.

• For $(V_\theta/V_t) < 4$, The UA numerical results for tornado path deviation shape are comparable to field observations (single and no curvature).

• The UA Numerical results for $(V_\theta/V_t) > 4$ are comparable to wind tunnel data (double curvature). Therefore the computer model can be considered for further investigation.

Only one topography configuration is considered in this study which is a ridge of height equal to the tornado radius. The ridge slope is 20%, and maximum considered (V_θ/V_t) ratio is 8. More investigation for different ridge height and slopes need to be examined for better understanding of this complicated phenomenon.

REFERENCES

[1] Ward, N. B., (1972). The Exploration of Certain Features of Tornado Dynamics Using a Laboratory model, Journal of the Atmospheric Sciences, Vol. 29,pp. 1194-1204.

[2] Davies-Jones, R. P. (1973).The Dependence of Core Radius on Swirl Ratio in a Tornado Simulator, Journal of the Atmospheric Sciences,Vol. 30, pp. 1427-1430.

[3] Jischke, M. C., & Light, B. D. (1983). Laboratory simulation of tornadic wind loads on a rectangular model structure. Journal of Wind Engineering and Industrial Aerodynamics, 13(1), 371-382.

[4] Haan, F. L., Sarkar, P.P., and Gallus, W.A. (2008). Design, Construction and Performance of a Large Tornado Simulator for Wind Engineering Applications, Engineering Structures, Vol.30, pp. 1146–1159.

[5] Selvam, R. P. (1993). Computer Modeling of Tornado Forces on Buildings. Proceedings: The 7th US National Conference on Wind Engineering, Edited by: Gary C. Hart, Los Angeles, June 27-30, 605-613.

[6] Selvam, R. P., & Millett P. C. (2003). Computer modeling of tornado forces on buildings. Wind and Structures, 6, 209-220

[7] Gorecki, P. M., & Selvam, R. P. (2014). Visualization of tornado-like vortex interacting with wide tornado-break wall. Journal of Visualization, 1-14.

[8] Selvam, R. P. & Ahmed, N. S. (2013). The Effect of Terrain Elevation on Tornado Path. Proceedings of 12th Americas Conference on Wind Engineering. Seattle, WA, USA.

[9] Lewellen, D. C. (2012) 4B. 1 "Effects of topography on tornado dynamics: a simulation study". 26th Conference on Severe Local Storms (5 - 8 November 2012) Nashville, TN, American Meteorological society https://ams.confex.com/ams/26SLS/webprogram/Paper211460.html

[10] Karstens, C. D., Gallus, W.A, Jr., Sarkar, P.P, Lee, B.D., and Finley, C, A., (2012). "Understanding terrain impacts on tornado flow through tree-fall analysis of the joplin and tuscaloosa-birmingham tornadoes of 2011 and through numerical and laboratory vortex simulations". 26th Conference on Severe Local Storms (5 - 8 November 2012) Nashville, TN, American Meteorological society https://ams.confex.com/ams/26SLS/webprogram/Paper211978.html

[11] Karstens, C. D., (2012). Observations and Laboratory Simulations of Tornadoes in Complex Topographical Regions. PhD Dissertation, Department of Meteorology, Iowa State University.

[12] Selvam, R. P., Ahmed, N. S., Yousof ,M.A, Strasser, M, and Ragan, Q. (2014).Study of Tornado-Terrain Interaction from Damage Documentation of April 27, 2014 Mayflower, AR Tornado. Department of Civil Engineering, University of Arkansas, Fayetteville,AR 72701.

[13] NWS (2011).National Weather Service Weather Forecast Office. [2011]. Tuscaloosa-Birmingham Tornado. Retrieved October 7, 2014, from http://www.srh.noaa.gov/bmx/?n=event_04272011tuscbirm

[14] NOAA (2011). Tornado Information,' accessed 10 January2013, http://www.noaanews.noaa.gov/2011_tornado_ information.html

[15] NASA (2014). National Aeronautics and Space Administration. Tornado Damage in Mayflower, Arkansas : Image of the Day. Retrieved October 7, 2014, from http://earthobservatory.nasa.gov/IOTD/view.php?id=83612

[16] NWS (2014).National Weather Service Weather Forecast Office. [2014]. NWS Little Rock, AR. Retrieved October 7, 2014, from http://www.srh.noaa.gov/lzk/?n=pns043014txt.htm

[17] Lewellen, W. S. (1976). Theoretical models of the tornado vortex", Proceedings of the Symposium on Tornadoes, Edited by: R.E. Peterson, Texas Tech University, Lubbock, June 22-24, pp. 107-143.

[18] Selvam R.P., & Millett, P.C. (2005). Large Eddy Simulation of the Tornado-Structure Interaction to Determine Structural Loadings", Journal of Wind Engineering and Structures, Vol. 8,pp. 49-60.

[19] Selvam, R.P. ,(1997). Computation of Pressures on Texas Tech Building Using Large Eddy Simulation, J. Wind Engineering and Industrial Aerodynamics, 67 & 68, 647-657

[20] de Sampio, P.A.B, Lyra, P.R.M., Morgan, K. and Weatherill, N.P., (1993). Petro-Galerkin solutions of the incompressible Navier-Stokes equations in primitive variables with adaptive remeshing, Computer Methods in Applied Mechanics and Engineering, 106, 143-178.

[21] Selvam, R.P. and Paterson, D.A., (1993). Computation of Conductor Drag Coefficients, J. Wind Engineering and Industrial Aerodynamics, 50, 1-8.

[22] Tamura, T. E. T. S. U. R. O., Itoh, Y., Wada, A., & Kuwahara, K. (1995). Numerical study of pressure fluctuations on a rectangular cylinder in aerodynamic oscillation. Journal of wind engineering and industrial aerodynamics, 54, 239-250.

[23] Tamura, T. (1999). Reliability on CFD estimation for wind-structure interaction problems. Journal of Wind Engineering and Industrial Aerodynamics, 81(1), 117-143.

[24] Selvam, R.P., (1998). Computational procedures in grid based computational bridge aerodynamics, in Bridge Aerodynamics, Larsen, A. and Esdahl (eds), Balkema, Rotterdam, pp. 327-336.

[25] Selvam, R.P. and Peng, Y., (1998). Issues in computing pressure around buildings, in Structural Engineering World Wide 1998, N.K. Srivastava (eds), Elsevier, New York, pp: 941, Paper reference T171-3.

[26] Sarkar, S., & Selvam, R. P. (2009). Direct Numerical Simulation of Heat Transfer in Spray Cooling Through 3D Multiphase Flow Modeling Using Parallel Computing. Journal of Heat Transfer, 131(12), 121007.

[27] Pielke, RA., (1984), Mesoscale Meterological Modeling. Academic Press, 612 pp.

[28] Selvam, R. P., & Rao, K. S. (1996). WINDFCT: A mass consistent wind field model for complex terrain (No. CONF-960127--). American Meteorological Society, Boston, MA (United States).

[29] Fujita, T. T. (1989). The Teton-Yellowstone tornado of 21 July 1987. Monthly Weather Review, 117(9), 1913-1940.

[30] CAP (2014). Civil Air Patrol Images. (2014, September 25). ArcGIS. Retrieved October 7, 2014, from http://www.arcgis.com/home/webmap/viewer.html?useExisting=1